Composite Structures 267 (2021) 113851

Contents lists available at ScienceDirect

Composite Structures

journal homepage: www.elsevier.com/locate/compstruct

Parametric sizing study for the design of a lightweight composite railway axle

Preetum J. Mistry [a,*], Michael S. Johnson [a], Shuguang Li [a], Stefano Bruni [b], Andrea Bernasconi [b]

[a] Composites Research Group, Faculty of Engineering, University of Nottingham, Advanced Manufacturing Building, Jubilee Campus, NG8 1BB, UK
[b] Department of Mechanical Engineering, Politecnico di Milano, Milan, Italy

ARTICLE INFO

Keywords:
Railway axle
Lightweighting
Composite material
Unsprung mass
Composite design
NEXTGEAR

ABSTRACT

The potential for lightweighting of railway axles was investigated to primarily reduce the unsprung mass of a rail vehicle. The reduction of unsprung mass equates to an overall lighter train which will help to reduce track damage, energy consumption and total operating costs. This work was performed within the NEXTGEAR project which is ascribed under the Shift2Rail program. This paper focusses on the design of a composite railway axle as part of the "Wheelset of the future" Work Package 3.

A parametric study is presented for the sizing of one of the design concepts (the full-length pre-manufactured tube axle) that shows the greatest potential for mass reduction. This study uses the existing hollow steel axle as a benchmark for mass, strength and stiffness. The estimated mass of this composite axle is 50 kg. This represents an estimated mass reduction of 75% compared to the existing hollow steel axle.

1. Introduction

The volume of European rail traffic is growing rapidly. This makes it ever-more important that tracks, signals, and bridges are both safe and reliable. Given the 221,000 km of track in Europe, this is an enormous task [1]. The cost of infrastructure maintenance and renewal already exceeds €25 billion a year across Europe, and this is continuing to rise. Despite this spending, operators are under pressure to maintain their assets. This results in unacceptably frequent delays, train cancellations and increased downtime for maintenance [2].

Compounding the reduced periods available for track maintenance is the gross mass of rail vehicles themselves. There is a current trend towards increasing mass of rail vehicles [3], having the effect of increasing axle loads. Heavier trains, running at higher speeds and greater density, have led to increased stresses on the rails. This results in rail wear and rolling contact fatigue which poses a significant risk to safe and reliable rail transport.

Lightweighting of rail vehicles is thus a necessity for reducing this damage and is also identified as a key enabler in reducing energy consumption [4]. The incorporation of polymer composites used for structural components is one means of providing lighter rail vehicles. The greatest proportion of mass of a rail vehicle is attributed to the rail bogie, constituting up to 41% of the mass [5]. A rail bogie contains several masses separated by suspension systems as shown in Fig. 1. The bogie is a chassis that contains the wheelsets and supports the rail vehicle body.

The wheelsets, comprising the axle and wheels, represent the majority of the unsprung mass which gives rise to track impact damage. A steel axle constitutes ~35% (198 kg) of a typical wheelset by mass, and this component has significant lightweighting potential. However, the axle is subjected to combined loading and undergoes rotating bending fatigue throughout its lifetime.

The challenge of lightweighting the unsprung mass is being addressed through the NEXTGEAR project [6], which is ascribed under the Shift2Rail Programme funded by the EU Horizon 2020 Research and Innovation Programme. One theme of NEXTGEAR is the "Wheelset of the Future". This comprises the design of a composite railway axle to form a hybrid metallic-composite (HMC) wheelset. The aim is to reduce the unsprung mass of the bogie with a focus on the design of a composite railway axle. This paper presents a parametric study for the sizing of the full-length pre-manufactured tube axle design concept.

2. Lightweighting of the unsprung mass

A number of research programmes to address bogie lightweighting, through the implementation of fibre reinforced polymer (FRP)

* Corresponding author.
E-mail addresses: preetum.mistry@nottingham.ac.uk (P.J. Mistry), michael.johnson@nottingham.ac.uk (M.S. Johnson), shuguang.li@nottingham.ac.uk (S. Li), stefano.bruni@polimi.it (S. Bruni), andrea.bernasconi@polimi.it (A. Bernasconi).

https://doi.org/10.1016/j.compstruct.2021.113851
Received 7 September 2020; Revised 29 January 2021; Accepted 13 March 2021
Available online 19 March 2021

Nomenclature

$P_{journal}$	Load acting on journal (N)
P_{wheel}	Reaction force of wheel exerted on axle (N)
F_f	Wheel pull off load (N)
MX	Sum of bending moments in x-direction (Nmm)
MY	Sum of torsional moments in y-direction (Nmm)
MZ	Sum of bending moments in z-direction (Nmm)
MR	Resultant bending moment (Nmm)
N_y	Combined plate loading intensity in the x-direction (Nmm)
N_y^{axial}	Axial load intensity (Nmm)
$N_R^{bending}$	Bending load intensity (Nmm)
N_{xy}	Torsional load intensity (Nmm)
p_i	External compressive pressure load (MPa)
p_{ii}	Internal compressive pressure load (MPa)
σ_R	Bending stress (MPa)
σ_r	Radial stress (MPa)
σ_c	Circumferential stress (MPa)
σ_{vM}	Von Mises stress (MPa)
$D_{o,b}$	Outer diameter of steel axle body (mm)
$D_{o,w}$	Outer diameter of steel axle wheel seat (mm)
D_i	Inner diameter of steel axle (mm)
D_h	Outer diameter of steel wheel hub (mm)
$d_{o,c}, d_{o,p}, d_{o,s}$	Outer diameter of the metallic collar, primary composite tube and secondary composite tube respectively (mm)
$d_{i,c}, d_{i,p}, d_{i,s}$	Inner diameter of the metallic collar, primary composite tube and secondary composite tube respectively (mm)
t_c, t_p, t_s	Thickness of the metallic collar, primary composite tube and secondary composite tube respectively (mm)
t	Laminate thickness (mm)
$t_0, t_{\pm 45}, t_{90}$	Thickness of 0°, ±45° and 90° plies (mm)
$n_0, n_{\pm 45}, n_{90}$	Number of 0°, ±45° and 90° plies
l_c, l_p, l_s	Length of the metallic collar section, primary composite tube and secondary composite tube respectively (mm)
L_b	Length of steel axle body (mm)
L_w	Length of steel wheel seat (mm)
L_a	Length of axle (mm)
L	Distance between the load on the wheels measured along the centreline (mm)
a	Distance between the centreline of the load on the journal and the centreline of the reaction of the wheel (mm)
j	Interference value for press-fitting wheel onto axle (mm)
δ_{max}	Maximum deflection (mm)
δ_i	Radial displacement (mm)
u_r	Radial inner displacement (mm)
E_x	Stiffness of composite layup (GPa)
I	Second moment of area (mm^4)

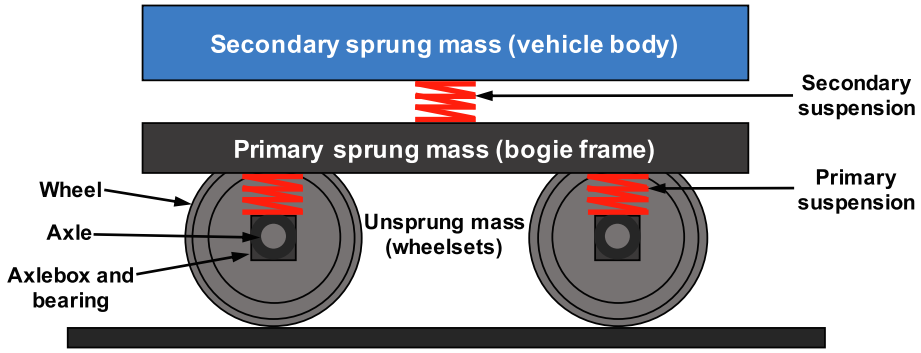

Fig. 1. The mass breakdown and sprung environments of a rail vehicle bogie with outboard bearing wheelsets.

composites have been undertaken. These programmes focussed mainly on the bogie frame structure. Two of the most significant examples include; the Carbon Fibre Bogie (CaFiBo) project developed by the University of Huddersfield, currently undergoing full scale testing [7], and the CRRC carbon fibre metro vehicle, "CETROVO", with a carbon-fibre bogie frame [8]. Both composite bogie frames cite an approximate 40% mass savings when compared to the metallic bogie frame.

In terms of rail wheelset lightweighting, a feasibility study relating to a freight wagon has been published [9]. However, only one prototype axle project is available in the literature. This was led by British Rail in the UK, addressing lightweighting of a rail axle (see Fig. 2). British Rail investigated the use of carbon fibre reinforced polymer (CFRP) composites for rail vehicle axles during development of the Advanced Passenger Train (APT) [10].

The initial concept showed a potential mass savings of 70% using the composite tube in comparison to the steel axle with a behaviour determined as being satisfactory in both static and fatigue tests [10]. However, the impact behaviour of the composite tube was found to be poor. Batchelor concluded that substantial benefits could be achieved

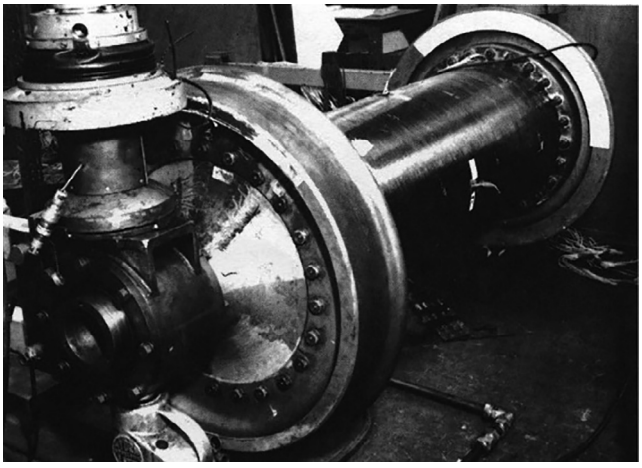

Fig. 2. Composite rail vehicle axle developed by British Rail for the experimental Advanced Passenger Train, 1981 [10].

by incorporating composites into railway wheelsets with further research and development. Beyond the APT programme in 1981, no other composite rail axle prototype has been reported in the literature.

3. Case study wheelset and axle

There are two main wheelset configurations: inboard and outboard bearing wheelsets as shown in Fig. 3. The general loading requirements for the outboard bearing wheelset architecture are cited in Standard EN 13103-1 [11], whereas the inboard architecture follows Standard BS 8535 [12].

An outboard solution provides a greater overall wheelset weight savings when going from (high density) steel to (high strength-to-weight ratio) composite, by virtue of it being a longer axle having more material. In addition, the outboard solution affords greater design freedom. A larger space envelope is available for the axle and the "free" space between the wheels is likely to be greater. However, the literature suggests that low track force bogies typically have an inboard bearing configuration providing a lighter overall bogie assembly [13]. In addition, the structural requirements are less demanding. As a result, the inboard bearing wheelset, with a composite axle is selected as the focus of this study.

An inboard bearing trailer wheelset with a hollow, steel axle is used as a case study (Fig. 4). The plain shaft section, inboard of the bearings, is the prime design space of the axle for a composite substitution. The axle material is EA1N grade steel and the mass of the axle is 198 kg.

4. Design concepts

Several design concepts were developed for the composite railway axle design. These concepts rely on carbon fibre as the reinforcing structural material with epoxy resin as the binding matrix. This combination provides good reliability for this fatigue driven design. The distinction between concepts is largely dictated by the manufacturing method employed. The materials and manufacturing techniques are established technology.

For this parametric study, the concept of a full-length pre-manufactured tube axle (see Fig. 5) was chosen for this purpose since it was shown to provide superior mass savings.

This concept has a primary composite tube which has a length of the full axle. Roll wrapping is a possible manufacturing route for the tube. Either end of the composite tube would be fitted with identical, adhesively bonded, thin walled collars for mounting of the inboard bearings and wheels. The central region of the axle has a secondary composite tube roll wrapped over the primary composite tube to increase the axle diameter up to a thickness sufficient to support the loading requirements. The rationale of this concept is to minimise the mass of the assembly. This concept has a mass of 80 kg which is a 60% mass savings compared to the original steel axle.

5. Parameters for design

This section summaries the principal load cases and material inputs used in the parametric sizing study.

5.1. Load cases

The candidate inboard bearing trailer axle was designed using the method prescribed in the Standard BS 8535 [12], by considering a maximum axle load of 12 tonnes. This equates to a load, P, of 6 tonnes at each bearing under static load. The standard specifies two main load cases that are considered when investigating the structural behaviour of the axles:

- Load case 1 – Mechanical braking and straight track.
- Load case 2 – Mechanical braking and low speed curving.

A third load case associated with the wheel to axle fit is defined in the Standard BS EN 13260 [14]:

- Load case 3 – Wheel pull-off, F_f.

The resulting moments and forces relative to the global coordinate system for the critical ultimate loading case are shown in Fig. 6.

5.2. Material selection

The axle experiences up to 3.4×10^9 rotating bending fatigue cycles in a 30-year life span. However, fatigue testing of composite materials up to the giga-cycle regime is not well documented. Work by Michel, S. et al. [15], suggests that after 10^9 cycles the material strength of AS4/PEEK, a carbon fibre reinforced thermoplastic composite, degraded by between 40% and 90% from the initial strength values based on tension–compression fatigue. Furthermore, no endurance limit was determined.

However, the fatigue behaviour for composites up to 10^7 cycles is more readily accessible. Specific data on the material properties of fibre reinforced composites can be sourced from the Cambridge Engineering Selector (CES) EduPack software of Granta Design Limited [16]. Since the material, EA1N grade railway steel, is not present in the CES database an equivalent, 'Carbon steel, AISI 1030, normalised' is used.

This data at ambient conditions indicates that the fatigue strength of Epoxy-CF composites reduces by approximately 40% at 10^7 cycles while the EA1N equivalent grade steel reduces by 49% at the same level of cycling. The fatigue performance of the Epoxy-CF is expected to reduce more significantly when subjected to aggressive thermal and moisture conditions. As a guide, a 50% reduction of the ultimate static tensile and compressive strength is estimated as the fatigue endurance limit for 10^7 cycles for this parametric study.

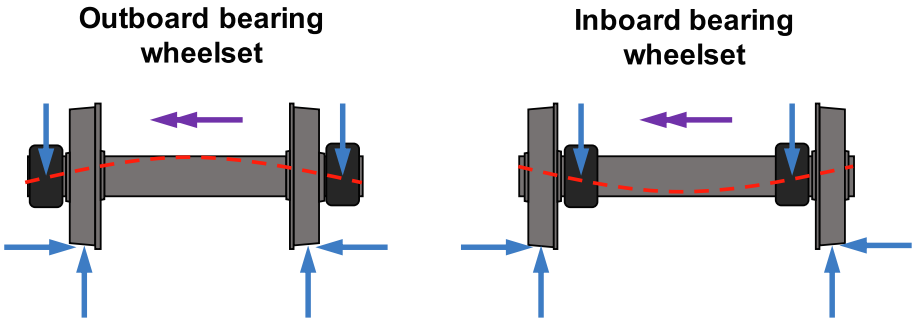

Fig. 3. Comparison of an inboard and outboard bearing wheelset configuration. Forces acting on the bearings and wheels (shown in blue), torque in the axle (shown in purple) and deflection of axle (shown in red).

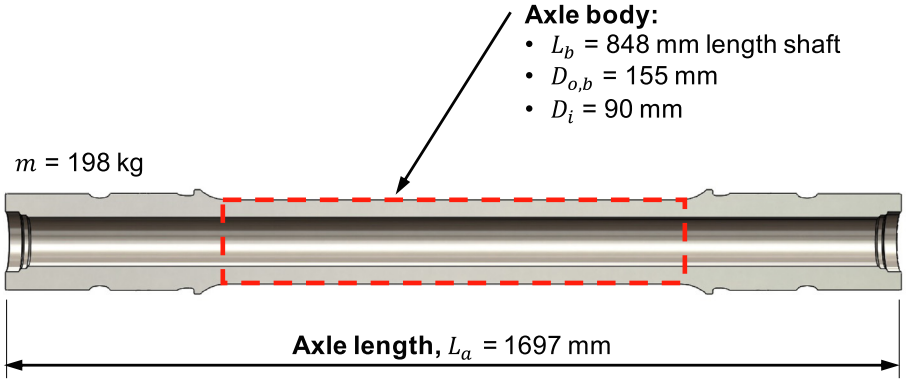

Fig. 4. Case study inboard bearing hollow steel axle forming a trailer wheelset (Source: Lucchini RS).

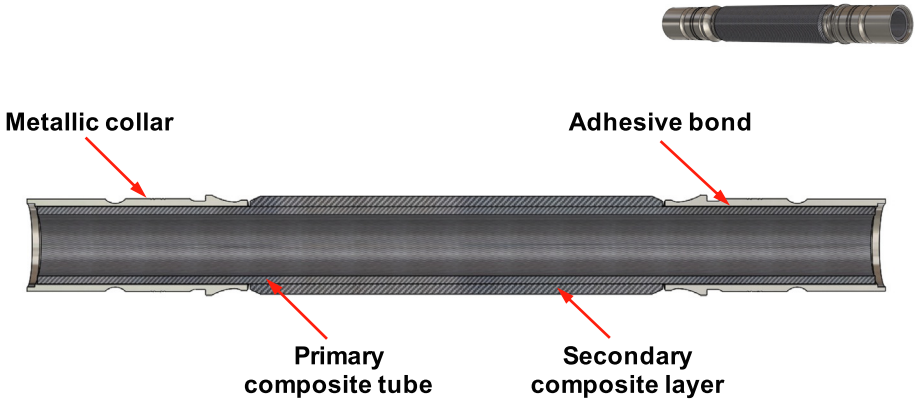

Fig. 5. Illustration of the full-length pre-manufactured tube axle concept for a rail vehicle.

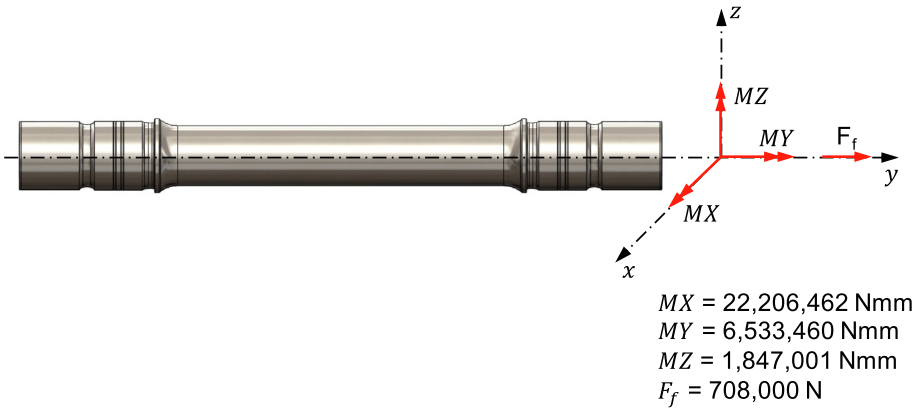

Fig. 6. Summary of the critical ultimate loading case relative to the global coordinate system.

The material properties are listed in the Appendix. The existing hollow steel axle and wheel are represented as AISI 1030 steel. Gurit UCHM450 SE 84LV unidirectional epoxy prepreg is used for the composite tube design. The collars are made from Ti-6Al-4V titanium alloy, as reasoned in Section 6.1.

5.3. Benchmark hollow steel axle design

The case study, hollow steel axle is in widespread use across the rail industry. As a result, it is certificated against Standard BS 8535 [12], with regard to performance. This Standard provides a basis for the composite axle design. Bending stress dominates in conventional loading with a significant normal stress developing from the wheel pull-off case. Simple and transverse shear stresses occur under static loading with torsional shear evolving primarily under braking conditions. Unlike a shaft used for torque transmission, the railway axle is dominated by the combined bending moments, *MX* and *MZ* (Fig. 6), rather than the torsional moment, *MY*, as clarified within the Standard. More specifically, it is the fully reversed fatigue loading derived from the bending moments that primarily lead to failure of a railway axle [17]. Buckling under combined bending and torsion at the middle section of the axle is discounted as the slenderness ratio (length/diameter) of the composite axle will be less than 10, and include a relatively thick wall.

While all load cases require careful consideration at the detailed design stage, particularly for the composite axle, this parametric study addresses mainly the strength and stiffness requirements due to the bending moments, as recommended by Standard BS 8535 [12].

5.3.1. Nominal sizing of the axle body – bending strength

The axle body ($D_{o,b}$ = 155 mm and D_i = 90 mm) comprises a plain diameter section occurring between the inboard bearing journals. The nominal sizing of which is based upon consideration of the resultant bending strength, arising from the resultant bending moment, and then determination of the strength reserve factor.

The bending stress, σ_R, on the outer diameter (OD) of the axle body can be defined from beam bending theory [18].

$$\sigma_R = \frac{MR \cdot y}{I}$$
$$\text{where, } y = D_{o,b}/2 \text{ and } I = \frac{\pi}{64} \cdot (D_{o,b}^4 - D_i^4) \quad (1)$$

The resultant bending moment, *MR*, is found by summing the bending moments experienced by the axle from load case 2.

$$MR = \sqrt{MX^2 + MZ^2} \quad (2)$$

The reserve factor of the hollow steel axle is calculated from the fatigue strength of steel at 10^9 cycles ($\sigma_{St,fat10^9}$) which is assumed to be 200 MPa (endurance limit) for EA1N grade steel as stated in Standard BS 8535 [12]. Therefore, the reserve factor, RF, for the bending strength can be determined.

$$RF = \frac{\sigma_{St,fat10^9}}{\sigma_R} = \frac{200\ MPa}{68.8\ MPa} = 2.91$$

Therefore, a bending strength reserve factor of 2.91 will be ensured for the composite axle design.

5.3.2. Nominal sizing of the axle body – stiffness

Consideration is given in the design of the axle to the stiffness as it determines the deflection. Management of the axle deflection is important for a several reasons: to ensure the bearings will tolerate the angular misalignment, the shaft whirl modes will be constrained and the fibre strains are minimised. Low fibre strains are necessary to inhibit crack development under high cycle fatigue.

The axle loading represents a beam in four-point bending as shown in Fig. 7.

The maximum deflection of the beam occurs at the centre span [18].

$$\delta_{max} = \frac{P \cdot a}{24 \cdot E \cdot I}\left[3 \cdot L^2 - 4 \cdot a^2\right]$$
$$\text{where, } I = \frac{\pi}{64} \cdot (D_{o,b}^4 - D_i^4) \quad (3)$$

where, a (172 mm), is the distance between the centre line of the load on the journal and the centre line of the reaction of the wheel. P, is the load or reaction force exerted on the axle. L (1500 mm), is the distance between the load on the wheels measured along the centreline. E, is Young's modulus of the material (EA1N grade steel, E_{St}) from which the axle is made and, I, is the second moment of area of the axle.

Therefore, the maximum deflection of the hollow steel axle can be calculated as, δ_{max} = 0.56 mm. This deflection should not be exceeded for the composite axle design.

5.3.3. Nominal sizing of the axle wheel seat – interference fit

The fitting of the wheel onto the axle is defined in Standard BS EN 13260 [14]. There is an interference fit between the axle wheel seat and the wheel hub bore. This determines the nominal sizing of the axle wheel seat. The interference value, j, to be adhered to for the press-fitting, is specified as a range in terms of mm.

$$0.0010 \cdot D_{o,w} \le j \le 0.0015 \cdot D_{o,w} + 0.06 \quad (4)$$

where, $D_{o,w}$, is the mean outer diameter of the axle wheel seat in mm (conventionally referred to as, d_m, in the Standard).

For the case study hollow steel axle, $D_{o,w}$ = 177 mm, the bore diameter, D_i = 90 mm and the length of the wheel seat, L_w = 150.85 mm as shown in Fig. 8.

Therefore, the interference values for press-fitting the wheel onto the axle can be determined.

$$0.1770\ mm \le j \le 0.3255\ mm$$

As a worst case, the maximum interference allowable between the inner wheel hub and the outer diameter of the axle wheel seat is, j = 0.3255 mm. This is the value that will be used in this sizing study.

A typical stress distribution through an open-ended cylinder when subjected to an external compressive pressure load, $-p_i$, is shown in Fig. 9.

The radial and circumferential stresses (σ_r and σ_c respectively) in the cylinder are always compressive. The maximum radial stress occurs at the OD of the cylinder ($D_{o,w}$ = 177 mm) and reduces to 0 at the ID of the cylinder (D_i = 90 mm). The circumferential stress is always greater than the radial stress, with its lowest value at the OD, increasing to a maximum at the ID. As the wall thickness reduces, the radial stresses remain the same ($-p_i$ at $D_{o,w}$, and 0 at D_i), but the

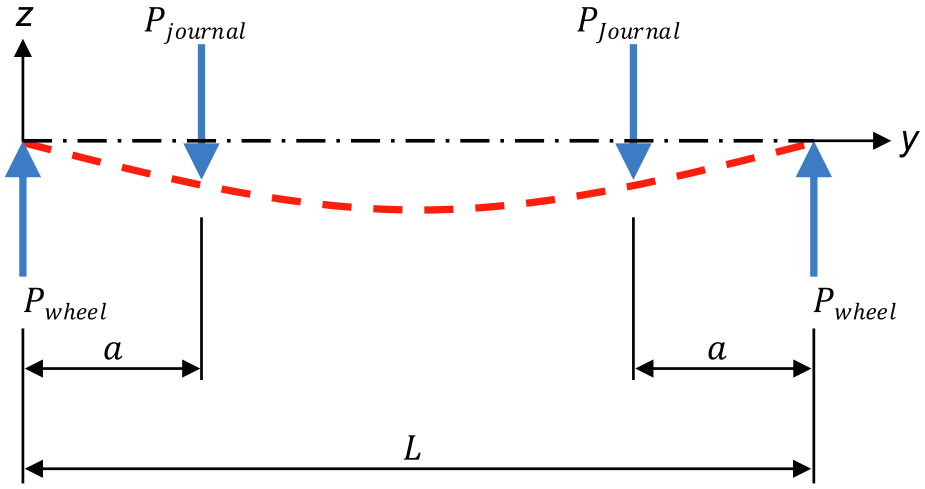

Fig. 7. Inboard bearing configuration of a non-powered, hollow axle, rail wheelset under static loading conditions (modelled as a beam in four-point bending).

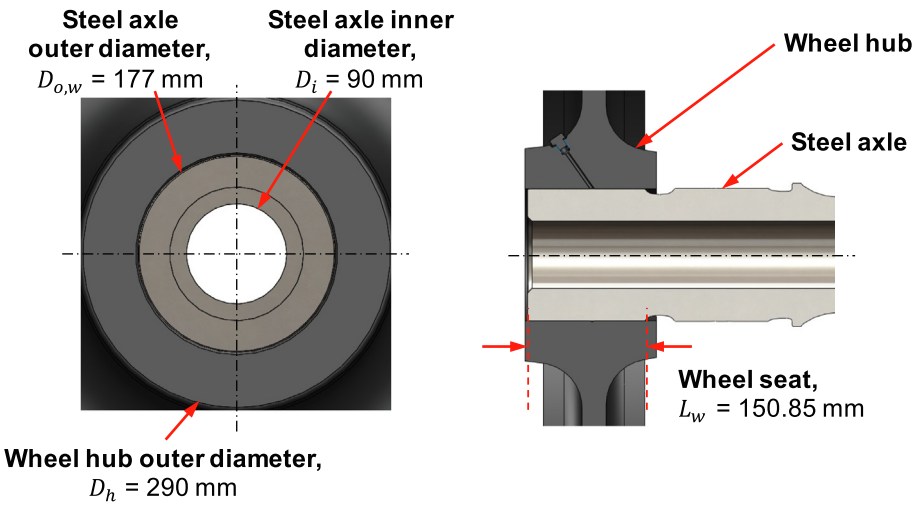

Fig. 8. Wheel hub press-fit onto hollow steel axle.

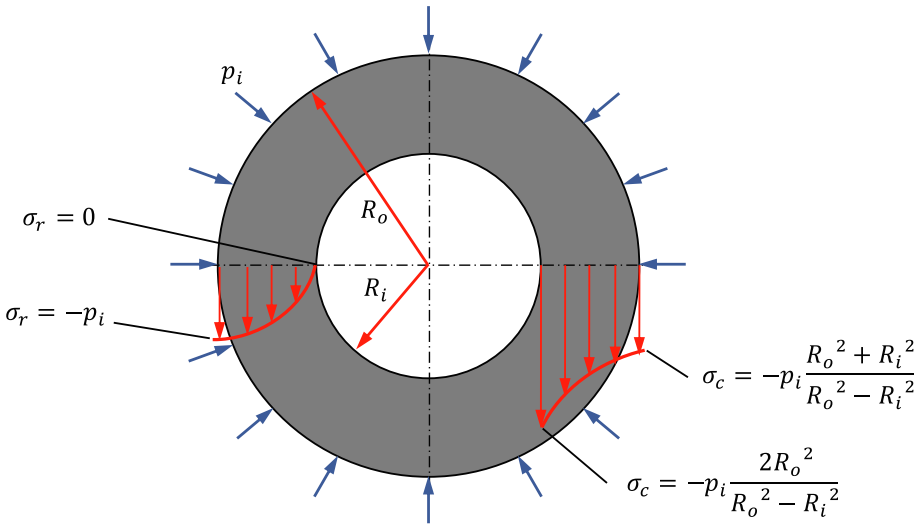

Fig. 9. Stress distribution in the radial and circumferential directions through a cylinder subjected to an external pressure load.

circumferential stresses on both OD and ID of the cylinder increase. In summary, reducing the wall thickness increases the circumferential stresses only with the maximum stress (circumferential) occurring at the ID of the cylinder.

In order to determine the reserve factor that the case study hollow steel axle has been designed to, the following calculation is performed.

The pressure, p_i, applied onto the steel axle as a result of the interference fit with the wheel hub is defined below [10]:

$$p_i = \frac{E_{St} \cdot j}{2 \cdot D_{o,w}^3} \cdot \left[\frac{\left(D_h^2 - D_{o,w}^2\right) \cdot \left(D_{o,w}^2 - D_i^2\right)}{D_h^2 - D_i^2} \right] \tag{5}$$

This clamping pressure is used to calculate the compressive radial and circumferential stresses. These stresses are combined using the von Mises (distortion-energy) failure theory. The assumption is that EA1N grade steel is ductile and has a maximum tensile strength comparable to the maximum compressive strength.

For the hollow steel axle case, press-fitting the wheel onto the axle will produce a von Mises stress, σ_{vM}, in the axle at the hub-axle interface of 140 MPa. This stress is less than the yield strength, $\sigma_{St,y}$, of the axle (EA1N grade steel) of 345 MPa, resulting in the following reserve factor against compressive failure.

$$RF = \frac{\sigma_{St,y}}{\sigma_{vM}} = \frac{345\ MPa}{140\ MPa} = 2.47$$

This reserve factor ensures that the interference fit is maintained so that the required torque can be sustained without slip and will be used for the composite railway axle.

The maximum compressive stress will arise at the ID of the hollow axle bore (D_i = 90 mm). At this location, the radial stress is zero, but the circumferential stress, σ_{c,D_i} = 255 MPa. The reserve factor against compressive stress is:

$$RF = \frac{\sigma_{St,y}}{\sigma_{c,D_i}} = \frac{345MPa}{255MPa} = 1.35$$

This reserve factor ensures that the hollow steel axle will not yield at the bore and this RF will be maintained for the composite railway axle.

6. Parametric sizing study of the composite axle

In order to refine the chosen design concept, a parametric sizing study is carried out to define the nominal geometry of the axle components. The design of the composite axle is benchmarked against the

hollow steel axle design in order to satisfy the strength, stiffness and axle compressive load from the wheel press-fit requirements.

The parametric study proceeds from:

- Sizing the metallic collars of the composite axle design.
- Determining the primary composite tube thickness and hence layup.
- Considering the deflection requirement and determining the secondary tube thickness and layup.

6.1. Composite axle design – metallic collars

A like for like replacement of a steel axle for a composite axle may seem like the most obvious solution for maximum lightweighting. However, fitting the metallic wheel directly onto a full composite axle would be impractical for a number of reasons. These include: issues achieving the required tolerances, preventing damage to the composite axle during wheel assembly and ensuring that the composite axle does not undergo a viscoelastic relaxation over a period of time. Therefore, keeping the metallic wheel/bearing seat contact is most important. For this reason, the chosen design concept proposes a metallic collar to be bonded to the OD of the composite axle such that the existing surface geometry defined by the steel axle is maintained.

The design principle is to contain the majority of radial and circumferential stresses associated with the interference fit of the wheel and bearing within the collar as opposed to transmitting those stresses into the composite axle. This is to be achieved in conjunction with maintaining a $RF \geq 2.47$ at the hub to collar interface and a $RF \geq 1.35$ at the ID of the collar. It follows that a metal with a higher yield strength than the EA1N grade steel ($\sigma_{St,y} = 345$ MPa), must be used for the collar to achieve these reserve factors while maintaining the same outer diameter, $D_{o,w}$, of 177 mm. As a result, Titanium 6Al-4 V ($\sigma_{Ti,y} = 850$ MPa), used commonly in the aerospace industry, is chosen for this purpose.

6.1.1. Superposition principle of tri-layer thick-walled cylinders

This design concept comprises of three concentric tubes; the wheel hub, the metallic collar and the hollow primary composite axle. The analytical approach outlined by Qiu and Zhou for this multi-layered configuration is used [19]. The method is described as an "outside to inside" superposition of three concentric thick-walled cylinders illustrated in Fig. 10. Here the interference fit is made between the wheel hub and metallic collar based upon the Standard BS EN 13260 [14]. Next, the hub and collar assembly are mated with the composite axle.

Radii numbered 1 to 4 are used in this section to refer to the geometry of the cylinders. r_1, refers to the OD of the wheel hub, r_2, refers to the OD of the metallic collar, r_3, refers to the OD of the primary composite tube and r_4, refers to the ID of the primary composite tube.

The pressure, p_i, associated with the wheel hub contracting onto the collar is determined as:

$$p_i = \frac{\delta_i}{r_2 \cdot \left[\frac{r_2^2\cdot(-1+\nu_1)}{E_1\cdot(-r_1^2+r_2^2)} + \frac{r_1^2\cdot(1+\nu_1)}{E_1\cdot(r_1^2-r_2^2)} - \frac{r_2^2\cdot(-1+\nu_2)}{E_2\cdot(r_2^2-r_3^2)} + \frac{r_3^2\cdot(1+\nu_2)}{E_2\cdot(r_2^2-r_3^2)}\right]} \tag{6}$$

As indicated in Fig. 10, the moduli are associated with the different materials for hub, collar and composite cylinders. The radial displacement, δ_i, is calculated by halving the interference fit between the wheel hub and collar, j:

$$\delta_i = \frac{j}{2} \tag{7}$$

The radial inner displacement, u_r, at the ID of the collar, onto the OD of the composite tube, is determined as:

$$u_r|_{r=r3} = \frac{-2\cdot p_i \cdot r_3 \cdot r_2^2}{E_2 \cdot (r_2^2 - r_3^2)} \tag{8}$$

This inward displacement is resisted by the composite tube. Increasing the thickness of the composite tube will provide greater resistance to the displacement and increase the stresses in the collar. Disregarding temperature effects, the pressure, p_{ii}, on the composite tube resulting from the inward displacement of the collar is:

$$p_{ii} = \frac{u_r}{r_3 \cdot \left[\frac{r_3^2\cdot(-1+\nu_2)}{E_2\cdot(-r_2^2+r_3^2)} + \frac{r_2^2\cdot(1+\nu_2)}{E_2\cdot(r_2^2-r_3^2)} - \frac{r_3^2\cdot(-1+\nu_3)}{E_3\cdot(r_3^2-r_4^2)} + \frac{r_4^2\cdot(1+\nu_3)}{E_3\cdot(r_3^2-r_4^2)}\right]} \tag{9}$$

From this, the resulting radial and circumferential stresses and hence reserve factors, can be calculated at each interface between the concentric tubes.

6.1.2. Nominal sizing of metallic collars

The objective of sizing the collar thickness, t_c, is to minimise the mass whilst achieving a $RF \geq 2.47$ at the hub to collar interface and a $RF \geq 1.35$ at the ID of the collar, to maintain equivalence with the hollow steel axle. The OD of the collar is fixed at 177 mm to keep with the existing wheel mounting geometry.

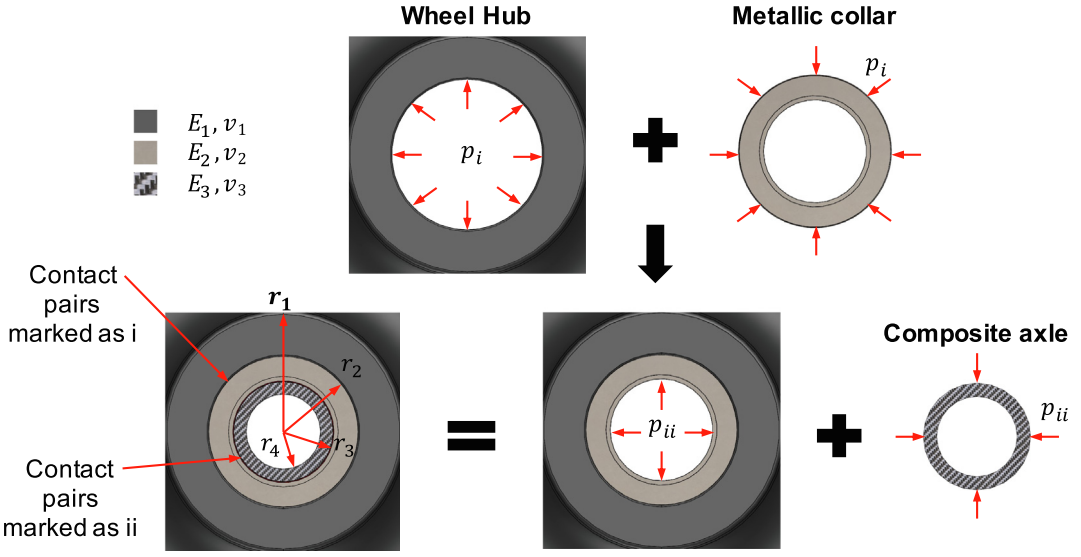

Fig. 10. Superposition principle of tri-layer thick-walled cylinders assembled from outside to inside. Here, E, is the Young's modulus and ν, is the Poisson's ratio. Subscript 1, refers to the wheel hub, subscript 2, refers to the metallic collar and subscript 3, refers to the primary composite tube.

Titanium 6Al-4V is chosen at a wall thickness of 12.5 mm (OD of 177 mm and ID of 152 mm). This is a practical thickness that would allow machining the OD at the wheel seat while leaving additional material for machining the stress relief features on either side. A unidirectional, CF-Epoxy prepreg with fibres oriented primarily along the axis of the axle is used (Gurit UCMH450 SE 84) for the primary composite tube. The OD of the primary composite tube is thus dictated by the collar thickness as 152 mm. However, the primary composite tube thickness is still to be determined.

6.2. Composite axle design – primary composite tube

By consideration of the bending strength requirement ($RF \geq 2.91$), the thickness of the primary tube can be sized, based on a fatigue strength of 50% of the longitudinal compressive strength, $\sigma_{11,c,fat10^7}$, of the composite (see Fig. 11).

Generally, a tube of thickness greater than 15 mm is likely to be difficult to manufacture without defects [20]. A reserve factor of 2.91 or above against bending strength is required for the axle design. The green highlighted area shows the ideal solution of tube OD and corresponding thickness. Based on the nominal collar sizing ($d_{o,c}$ = 177 mm, wall thickness, t_c, 12.5 mm) the OD of the primary composite tube is 152 mm. From Fig. 11, a conservative thickness for the primary composite tube is 12.5 mm. Therefore, the reserve factor for the bending strength can be determined.

$$RF = \frac{50\% \cdot \sigma_{11,c,fat10^7}}{\sigma_R} = \frac{421.7MPa}{126.1MPa} = 3.34$$

As this is greater than a reserve factor of 2.91, the tube thickness of 12.5 mm is acceptable.

6.2.1. Validation of the collar and primary composite tube sizings

Having sized the collar and primary composite tube as components, a reassessment of the compressive stresses in the assembly is undertaken. The nominal dimensions of these components are:

- Titanium alloy collar: OD of 177 mm and ID of 152 mm giving a wall thickness of 12.5 mm.
- Primary composite tube: OD of 152 mm and an ID of 127 mm giving a wall thickness of 12.5 mm.

Titanium collar:

- Reserve factor against the compressive stress in the collar, at the hub to collar interface (r_2 in Fig. 10):

$$RF = \frac{\sigma_{Ti,y}}{\sigma_{vM}} = \frac{850\ MPa}{181\ MPa} = 4.70$$

This is greater than the benchmark value, $RF \geq 2.47$.

- Reserve factor against the compressive stress in the collar, at the collar to primary composite tube interface (r_3 in Fig. 10):

$$RF = \frac{\sigma_{Ti,y}}{\sigma_{vM}} = \frac{850\ MPa}{194\ MPa} = 4.38$$

This is greater than the benchmark value, $RF \geq 1.35$.

Primary composite tube:

- Reserve factor against the compressive stress in the primary composite tube (r_3 in Fig. 10):

$$RF = \frac{\sigma_{22,c}}{\sigma_{max,c}} = \frac{83.1\ MPa}{11.7\ MPa} = 7.10$$

- Reserve factor against the compressive stress at the ID of the primary composite tube (r_4 in Fig. 10):

$$RF = \frac{\sigma_{22,c}}{\sigma_{max,c}} = \frac{83.1\ MPa}{13.6\ MPa} = 6.11$$

As the reserve factors against the compressive stress in the primary composite tube are greater than 1, failure is not expected to occur.

For completeness, the bending strength in the primary composite tube is assumed to be unaffected by the inclusion of the collar. Therefore, the reserve factor against the bending strength in the composite tube is 3.34 as calculated above.

It is now necessary to determine the layup for the primary composite tube and the additional secondary windings over the axle body to satisfy the stiffness requirements.

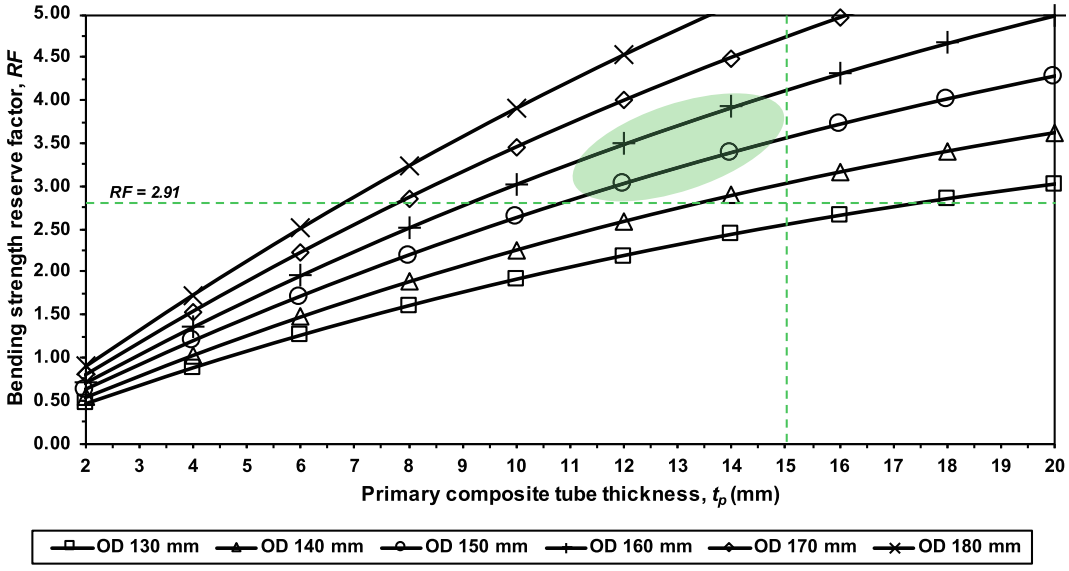

Fig. 11. Axle body reserve factor against primary composite tube thickness for a range of outer diameters (ODs) for 10^7 cycles (50% of σ_{UTS} based on 0° compressive strength).

6.2.2. Determine the layup of the primary composite tube

An empirical "netting strength" method, described by Barbero [21], is used to determine the approximate composite layup of the primary tube (OD of 152 mm and a wall thickness, t_p, of 12.5 mm) in terms of 0^0, $\pm 45^0$ and 90^0 plies to meet the load cases.

It is recognised that the final wall thickness will be dependent on the fatigue performance of the laminate. The fatigue strength at 10^7 cycles is used for the sizing calculation.

Step one – determine the plate load intensities, *N*

The axial load intensity is determined from the wheel pull-off load case 3.

$$N_y^{axial} = \frac{F_f}{\pi \cdot d_{o,p}} \tag{10}$$

The bending load intensity is from the bending moment $\left(MR = \sqrt{MX^2 + MZ^2}\right)$ acting on the axle, load case 2.

$$N_R^{bending} = \sigma_R \cdot t = \frac{\pm 32 \cdot MR \cdot d_o \cdot t_p}{\pi \cdot \left(d_{o,p}^4 - d_{i,p}^4\right)} \tag{11}$$

where, t, is the thickness of the laminate.

Hence, the combined plate loading intensity, N_y, can be calculated.

$$N_y = N_y^{axial} \pm N_R^{bending} \tag{12}$$

The torsional load intensity can be determined from the torque acting along the axle, from load case 2.

$$N_{xz} = \tau_{xz} \cdot t = \frac{16 \cdot MY \cdot d_o}{\pi \cdot \left(d_{o,p}^4 - d_{i,p}^4\right)} \tag{13}$$

As the simple and transverse shear stresses are considered higher order cases, the associated stress intensities are not considered in this analysis.

In summary the plate loading intensities are as follows:

$$\begin{Bmatrix} N_y \\ N_{xz} \end{Bmatrix} = \begin{Bmatrix} 3059\ N/mm \\ 231\ N/mm \end{Bmatrix} \text{ and}$$
$$\begin{Bmatrix} N_y \\ N_{xz} \end{Bmatrix} = \begin{Bmatrix} -93\ N/mm \\ 231\ N/mm \end{Bmatrix}$$

Step two – laminate "netting" design

Determine the number of 0° plies required in the layup by considering the thickness of that layer.

$$\sigma_y = \frac{N_y}{t_0} \le \sigma_1^*, \ \textit{therefore}\ t_0 \ge \frac{N_y}{\sigma_1^*} \tag{14}$$

where, σ_1^*, refers to the maximum tensile/compressive strength for the material in the longitudinal (0^0) direction ($\sigma_{11,t,fat10^7}$ and $\sigma_{11,cfat10^7}$). The number of 0° plies is calculated by dividing the thickness of 0° plies ($t_0 = 3.92$), by the cured ply thickness of the composite material ($t_{ply} = 0.45$ mm).

$$n_0 = \frac{3.92\ mm}{0.45\ mm} = 8.70$$

The same procedure is followed to determine the number of ±45° plies required in the layup by first determining the thickness of that layer ($t_{\pm 45} = 0.55$).

$$\sigma_{xz} = \frac{N_{xz}}{t_{\pm 45}} \le \sigma_1^*, \ \textit{therefore}\ t_{\pm 45} \ge \frac{N_{xz}}{\sigma_1^*} \tag{15}$$

where, σ_1^*, refers to the maximum compressive strength for the material in the longitudinal (0^0) direction ($\sigma_{11,cfat10^7}$). The thickness of the ± 45° plies is $t_{\pm 45} = 0.55$. The number of ± 45° plies required can be calculated.

$$n_{\pm 45} = \frac{0.55\ mm}{0.45\ mm} = 1.22$$

Step three – Final laminate

Based on general rules for determining composite layups, the results from step two are rationalised as:

- Round up to obtain an even number of plies.
- Include at least 10% of each orientation of plies in each direction.
- Consider symmetry and balance of ±45° plies.

Therefore, the required layup for the primary composite tube based on the minimum number of plies to satisfy the strength requirements are rounded up to the meet the 12.5 mm wall thickness estimated in the previous section. The 0° plies are rounded up from 8.70 to 16, the ±45° plies are rounded up from 1.22 to 4 and the 90° plies are rounded from 0 to 4.

$$\textit{primary composite tube layup} = \left[\pm 45^\circ, 0^\circ{}_2, 90^\circ, 0^\circ{}_2\right]_{2|s}$$

This equates to 28 plies and results in a primary composite wall thickness of 12.6 mm.

In summary:

- Titanium alloy collar: OD of 177 mm and ID of 152 mm giving a wall thickness of 12.5 mm.
- Primary composite tube: OD of 152 mm and an ID of 126.8 mm giving a wall thickness of 12.6 mm.

6.3. Composite axle design – secondary composite layer

The axle design, based on the primary composite tube, now meets the strength requirement. The next requirement to consider is stiffness. The deflection of the primary composite tube is determined by consideration of the composite thickness fractions used to determine the laminate stiffness of the axle body.

The stiffness of the composite layup, E_x, can be calculated using the "Netting stiffness" and "Hart-Smith 10%" rule and then averaged to find the approximate stiffness of the layup [21].

$$E_{x,netting} = \left(\frac{t_0}{t} \cdot E_{11,t}\right) + \left(\frac{t_{90}}{t} \cdot 0\right) + \left(\frac{t_{\pm 45}}{t} \cdot 0\right) \tag{16}$$

$$E_{x,H-S} = E_{11,t} \cdot \left[\left(\frac{t_0}{t} \cdot 1.0\right) + \left(\frac{t_{90}}{t} \cdot 0.1\right) + \left(\frac{t_{\pm 45}}{t} \cdot 0.1\right)\right] \tag{17}$$

The average stiffness of the composite axle body is calculated to be 123.47 GPa. The deflection of the hollow composite axle can be determined using Eq. (3).

The deflection of this composite axle (based on the primary composite tube) is, $\delta_{max} = 1.68$ mm (Eq. (3)). This deflection is much greater than that of the steel axle, $\delta_{max} = 0.56$ mm. The composite axle needs additional bending strength to increase the stiffness. The strategy for this will be to add 0^0 plies around the primary composite tube in the form of a roll wrapped secondary layer to provide additional stiffness. The results for this are shown in Fig. 12.

6.4. Recommended solution

The chosen design concept comprises a full-length composite tube (the primary axle) with an overwrapped (secondary) tube in the central region of the axle.

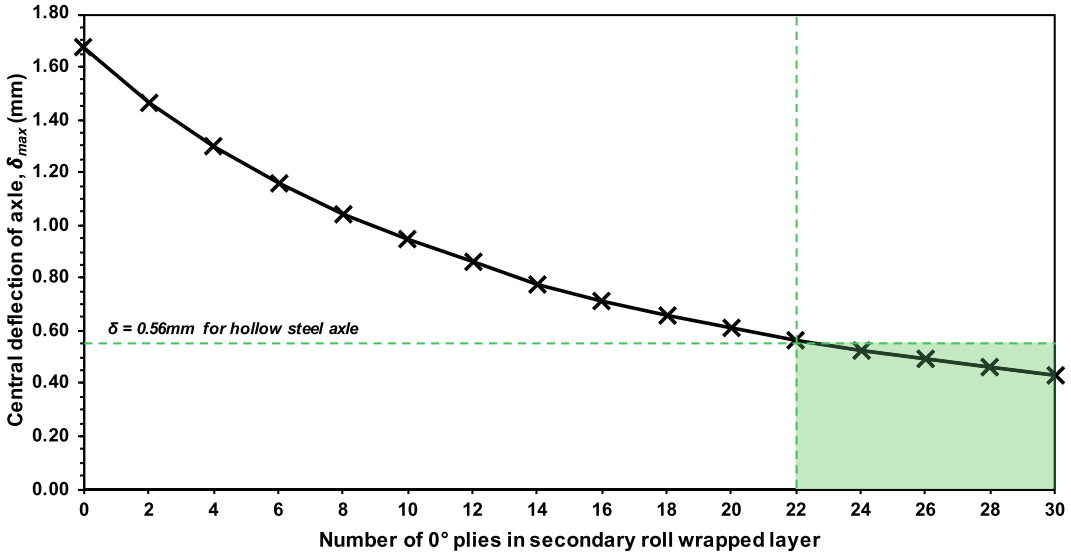

Fig. 12. Maximum central deflection of the composite axle (inner diameter of 126.8 mm) against increasing number of 0^0 plies in the secondary composite tube.

The primary tube has an ID of 126.8 mm and is 28 plies thick (0.45 mm per ply) giving a wall thickness of 12.6 mm. The OD is 152 mm. The primary tube includes a ± 45° layer on the inner and outer surfaces to accommodate torsional loading while providing shielding to the inner fibres.

The secondary tube primarily uses 0° fibres to provide bending stiffness. The ID of the tube is 152 mm and it is considered to be rigidly bonded to the OD of the primary tube. Ideally, there would be 24 off 0° plies in the secondary tube, but achieving an overall balanced laminate will result in an increased OD in the middle section.

For the primary composite tube, the main loading is bending. This requires 0° fibres along the axis of the tube. Catering for secondary loading, for example torsion and transverse shear, requires the use of ±45° fibres. The 90° fibres will provide a number of functions including:

- Hoop strength for reacting centrifugal forces that develop during axle rotation.
- Compressive strength to react the circumferential stresses in the collar region.
- Crack growth suppression along the 0° degree fibres.

The secondary composite tube layup considering "Rules of Thumb" for laminate design consists of 24 off 0° plies, 6 off ±45° plies and 6 off 90° plies.

$$\textit{Secondary composite tube layup} = \left[\pm 45^{\circ}, 0^{\circ}{}_2, 90^{\circ}, 0^{\circ}{}_2\right]_{3|s}$$

This equates to 42 plies and results in a primary composite wall thickness of 18.9 mm.

The recommended solution for this design concept of the composite axle is illustrated with the associated dimensions in Fig. 13.

The mass of the composite axle design can be calculated given the geometry of the individual components as shown in Fig. 13. The mass of the full-length pre-manufactured tube axle is 50 kg. The mass savings over the existing hollow steel axle (198 kg) can be compared.

$$\textit{Mass savings} \cong \frac{198\ kg - 50\ kg}{198\ kg} = 75\%$$

Therefore, an estimated mass savings of 75% can be achieved. This is in line with predictions from work conducted by Mistry and Johnson [22] who investigated the economic benefit of lightweight hollow composite railway axles. The authors estimated a potential 64% mass savings in a hollow composite axle compared to a hollow steel axle (outboard bearing configuration).

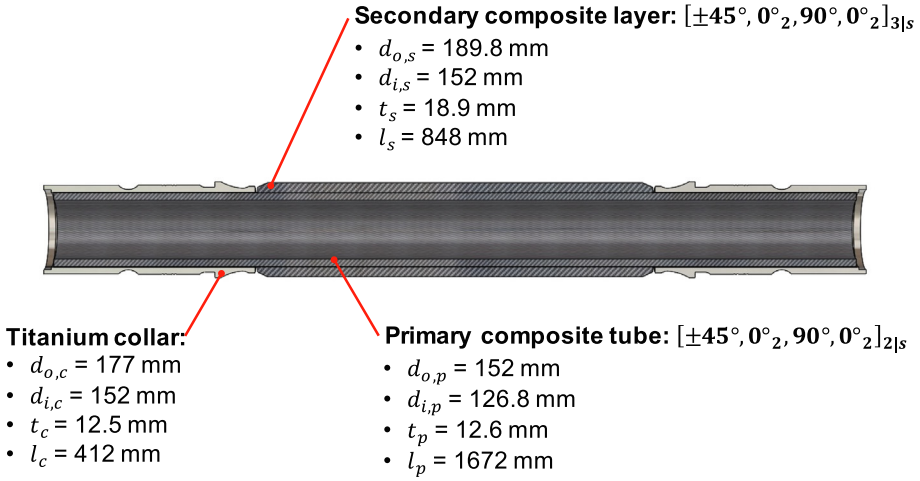

Fig. 13. Recommended solution for the full-length pre-manufactured tube axle design concept. Where, *d*, refers to the diameter of the tube, *t*, refers to the thickness of the section and *l*, refers to the length of the section.

The outcome of this parametric study is a recommended solution for the chosen design concept as shown in Fig. 13. This solution provides a weight savings of approximately 75% over the existing, hollow steel axle. This is a mid-fidelity concept solution based on the Standard BS 8535 [12]. However, this Standard assumes the material to be isotropic. As a result, the solution for an anisotropic composite requires a detailed analysis to be undertaken. This includes consideration of all the load cases beyond combined bending and torque. Definition of the laminate using Classical Lamination Theory (CLT) applying a failure criterion would increase confidence in the presented solution. Extension of the CLT solution to a Finite Element Analysis (FEA) would provide further confirmation and allow stress concentrations within the axle to be resolved.

7. Conclusions

This paper proposes a full-length pre-manufactured tube axle concept for the railway axle design. This concept shows the greatest potential for mass reduction. In order to raise the fidelity of this concept, a parametric study was performed.

The parametric study used the existing hollow steel axle as a benchmark for both strength and stiffness. The wheel seat and journal for the steel axle were maintained as interfacing geometry for the composite axle.

Unlike a shaft used for torque transmission, the railway axle is dominated by bending rather than by the torsional loading. More specifically, it is the fully reversed fatigue loading derived from the bending moments that primarily lead to failure. Axial and torsional loading has been considered. Simple and transverse shear have been confirmed by calculation as secondary load cases. Buckling under combined bending and torsion is discounted as the slenderness ratio (length/diameter) of the composite axle will be less than 10 and include a relatively thick wall. While all load cases require careful consideration at the detailed design stage, this parametric study addressed mainly the strength and stiffness requirements due to the bending moments, as recommended by Standard BS 8535.

Titanium collars bonded onto a full length primary composite tube were sized, principally to withstand the compressive stresses generated by press fitting the wheel onto the axle. The primary composite tube was sized to meet the strength requirements of the axle. Lastly, the central region of the axle was overwrapped with a second layer of composite to reduce the bending to the same level as that of the steel axle. The maximum diameter of the composite axle is 190 mm with an inner diameter of 127 mm. Full indication of the final design parameters for the concept are shown in Fig. 13.

The approximate mass of this composite axle is 50 kg. This represents a mass reduction of 75% compared to the existing hollow steel axle.

A detailed stress analysis of this composite axle is the subject of future work. In particular, stress concentrations arising between the titanium collar and secondary composite roll wrap require specific consideration. In addition, bonding of the titanium collars onto the primary composite axle may lead to detailed design alterations.

CRediT authorship contribution statement

P.J. Mistry: Conceptualization, Validation, Methodology, Writing - original draft. **M.S. Johnson:** Supervision, Conceptualization, Methodology, Writing - review & editing, Validation, Project administration. **S. Li:** Supervision, Writing - review & editing, Validation. **S. Bruni:** Project administration, Writing - review & editing. **A. Bernasconi:** Project administration, Writing - review & editing.

Declaration of competing interest

The authors declare that they have no known competing financial interests or personal relationships that could have appeared to influence the work reported in this paper.

Acknowledgements

This work was conducted as part of Work Package 3 of the NEXTGEAR Project, S2R-OC-IP1-02-2019 [Grant number: 881803], which is ascribed under the Shift2Rail Program funded by the EU Horizon 2020 research and innovation programme.

The authors would like to acknowledge the information regarding the benchmark inboard bearing, hollow steel axle provided by Lucchini RS, Italy.

The first author would like to acknowledge the funding support of the Engineering and Physical Sciences Research Council through the: EPSRC Future Composites Manufacturing Research Hub [Grant number: EP/P006701/1] and EPSRC Industrial Doctorate Centre in Composites Manufacture [Grant number: EP/L015102/1].

Appendix

Material properties used for the parametric sizing study of the composite railway axle.

Table A1. Mechanical properties of AISI 1030 Plain Carbon 0.3% Steel normalised (Source: Cambridge Engineering Selector Database).

Mechanical property	Symbol	Value	Unit
Young's modulus	E_{St}	200	GPa
Yield strength	$\sigma_{St,y}$	345	MPa
Poisson's ratio	ν_{St}	0.295	-
Density	ρ_{St}	7850	kg/m^3
Fatigue strength at 10^7 cycles	$\sigma_{St,fat10^7}$	270	MPa
Fatigue strength at 10^9 cycles	$\sigma_{St,fat10^9}$	200	MPa

Table A2. Mechanical properties of Titanium Ti-6Al-4V annealed (Source: Cambridge Engineering Selector Database).

Mechanical property	Symbol	Value	Unit
Young's modulus	E_{Ti}	115	GPa
Yield strength	$\sigma_{Ti,y}$	850	MPa
Poisson's ratio	ν_{Ti}	0.340	-
Density	ρ_{Ti}	4450	kg/m^3

Table A3. Mechanical properties of Gurit UCHM450 SE 84LV unidirectional (0°) laminate (Source: Gurit).

Mechanical property	Symbol	Value	Unit
Fibre volume fraction	v_f	56	%
Ply thickness	t_{ply}	0.45	mm
Ply weight	W_{ply}	683	g/m^2
Density	ρ	1498	kg/m^3
Longitudinal tensile modulus	$E_{11,t}$	208.26	GPa
Longitudinal tensile strength	$\sigma_{11,t}$	1562	MPa
Fatigue strength at 10^7 cycles (estimated)	$\sigma_{11,t,fat10^7}$	781	MPa
Longitudinal compressive modulus	$E_{11,c}$	187.43	GPa

(*continued on next page*)

(*continued*)

Mechanical property	Symbol	Value	Unit
Longitudinal compressive strength	$\sigma_{11,c}$	843.40	MPa
Fatigue strength at 10^7 cycles (estimated)	$\sigma_{11,c,fat10^7}$	421.7	MPa
Transverse tensile modulus	$E_{22,t}$	6.39	GPa
Transverse tensile strength	$\sigma_{22,t}$	28.80	MPa
Transverse compressive modulus	$E_{22,c}$	6.39	GPa
Transverse compressive strength	$\sigma_{22,c}$	83.1	MPa
Interlaminar shear modulus	E_{13}	4.31	GPa
Interlaminar shear strength	σ_{13}	64.70	MPa
In-plane shear modulus	E_{12}	4.31	GPa
In-plane shear strength (estimated)	σ_{12}	64.70	MPa
Poisson's ratio – longitudinal strain	ν_{12}	0.337	-

References

[1] Sixth report on monitoring development of the rail market. Report from the Commission to the European Parliament the Council: European Commission; 2019.
[2] Kienzler C, Lotz C, Stern S. Using analytics to get European rail maintenance on track. McKinsey & Company; 2020.
[3] Ford R. Transport mass: weight saving and structural integrity of rail vehicles. Derby, UK: Institution of Mechanical Engineers Seminar; 2007.
[4] Loubinoux J-P, Lochman L. Moving towards sustainable mobility: a strategy for 2030 and beyond for the European railway sector. Paris, France: International Union of Railways (UIC); 2012.
[5] Carruthers JJ, Calomfirescu M, Ghys P, Prockat J. The application of a systematic approach to material selection for the lightweighting of metro vehicles. Proc Inst Mech Eng, Part F: J Rail Rapid Transit 2009;223:427–37.
[6] NEXT generation methods, concepts and solutions for the design of robust and sustainable running GEAR (NEXTGEAR). S2R-OC-IP1-02-2019.
[7] Magma Structures. Composite rail vehicle bogie shows the future; 2019.
[8] CRRC. CRRC Announces Global Release of CETROVO Carbon-fibre Metro Vehicles; 2018.
[9] Good T, Hannema G, Paradies R, Shahverdi M. Towards noise and weight reduction by application of FRP wheelsets for freight cars; 2019.
[10] Batchelor J. Use of fibre reinforced composites in modern railway vehicles. Mater Des 1981;2(4):172–82.
[11] European Committee for Standardisation. Railway applications. Wheelsets and bogies. Part 1: Design method for axles with external journals. EN 13103-1:2017. Brussels, Belgium: CEN; 2017.
[12] British Standards Institution. Railway applications. Wheelsets and bogies. Powered and non-powered axles with inboard bearings. Design method. BS 8535:2011. London, England: BSI; 2011.
[13] Bracciali A, Megna G. Inside frame bogies & air wheelset a winning marriage. In: 10th International Conference on Railway Bogies and Running Gears. Budapest, Hungary. p. 12–5.
[14] British Standards Institution. Railway applications. Wheelsets and bogies. Wheelsets. Product requirements. BS EN 13260:2009+A1:2010. London, England: BSI; 2009.
[15] Michel S, Kieselbach R, Martens H. Fatigue strength of carbon fibre composites up to the gigacycle regime (gigacycle-composites). Int J Fatigue 2006;28(3):261–70.
[16] CES EduPack version 18.1.1. Copyright Granta Design Limited; 2018.
[17] Smith RA, Hillmansen S. A brief historical overview of the fatigue of railway axles. Proc Inst Mech Eng, Part F: J Rail Rapid Transit 2004;218:267–77.
[18] Budynas RG, Nisbett JK. Shigley's Mechanical Engineering Design. 9th ed. McGraw-Hill Higher Education; 2011.
[19] Qiu J, Zhou M. Analytical solution for interference fit for multi-layer thick-walled cylinders and the application in crankshaft bearing design. Appl Sci 2016;6(6):167. https://doi.org/10.3390/app6060167.
[20] Broughton W. Project CPD5 - Report 5: Thick Composites. National Physical Laboratory; 2001.
[21] Barbero EJ. Introduction to composite materials design. CRC Press; 2017.
[22] Mistry PJ, Johnson MS. Lightweighting of railway axles for the reduction of unsprung mass and track access charges. Proc Inst Mech Eng, Part F: J Rail Rapid Transit 2020;234:958–68.